Title

The Effects of Reduced Jmjd3 Expression on Muscle Regeneration Following Acute Injury

Author

Avila, Marcus A

Publication Date

2024

Peer reviewed|Thesis/dissertation

UNIVERSITY OF CALIFORNIA

Los Angeles

The Effects of Reduced Jmjd3 Expression on Muscle Regeneration Following Acute Injury

A thesis submitted in partial satisfaction of the requirements

for the degree Master of Science in Physiological Science

by

Marcus Andrew Avila

2024

ABSTRACT OF THE THESIS

The Effects of Reduced Jmjd3 Expression on

Muscle Regeneration Following Acute Injury

by

Marcus Andrew Avila

Master of Science of Physiological Science

University of California, Los Angeles, 2024

Professor James G. Tidball, Chair

The transition of muscle stem cells, known as satellite cells (SCs), from a quiescent state to an active, proliferative, and myogenic state facilitates muscle repair following injury. We tested the hypothesis that hemizygous expression of Jmjd3, a H3K27me3 histone demethylase, in SCs following acute injury would affect various stages of muscle regeneration. Our findings show there is an increased proportion of H3K27me2/3^{+}/Pax7^{+} cells out of total Pax7^{+} cells in acutely injured Jmjd3 hemizygous mice, suggesting the mutation reduced H3K27me2/3 demethylation. We next investigated muscle fiber growth and myonuclei per muscle fiber to determine myocyte fusion. Our data indicate the Jmjd3 mutation diminished the average cross-sectional area (CSA) of muscle fibers after injury, while having no effect on myonuclei per muscle fiber suggesting myocyte fusion was not affected. We then investigated myocyte proliferation and found the Jmjd3 hemizygous mutation reduced the proportion of Ki67^{+}/Pax7^{+}

cells out of total $Pax7^{+}$ cells, suggesting a reduction in injured muscle compared to Jmjd3 control mice. Our results show attenuation of H3K27me3 histone demethylation, muscle fiber growth, and SC proliferation when SC Jmjd3 expression is reduced, thus affecting muscle regeneration.

The thesis of Marcus Andrew Avila is approved.

Scott H. Chandler

Victor R. Edgerton

James G. Tidball, Committee Chair

University of California, Los Angeles

2024

Table of Contents

List of Figures

List of Tables

Introduction

Muscle repair and regeneration following acute injury are complex processes that involve coordinated molecular and cellular events. The events involved, known collectively as myogenesis, are regulated by myogenic regulatory factors that control muscle stem cell development and allow the generation of repaired or new muscle fibers. Expression of myogenic regulatory factors is closely regulated throughout the process of muscle repair and regeneration. Understanding the regulation of myogenesis is crucial for the development of new therapeutic approaches for the treatment of muscle injuries and diseases.

Myogenesis involves the activation and proliferation of muscle stem cells, differentiation of myoblasts into myocytes, and subsequent fusion or development of myocytes into mature muscle. Satellite cells (SCs), which are found between the basal lamina and sarcolemma of skeletal muscle fibers (Mauro, 1961), are a muscle stem cell population involved in early stages of myogenesis following injury. Satellite cells remain in a quiescent state until muscle tissue is perturbed, leading to their activation and proliferation (Cheng et al., 2008 & Maltzahn et al., 2013). During satellite cell proliferation, the daughter cells produced either return to quiescence to maintain the SC population or become active myoblasts geared towards muscle repair (Zammit et al., 2004). Myoblasts express specific regulatory factors that promote differentiation into myocytes that fuse together to form multinucleated cells known as myotubes. Myotubes form alongside damaged muscle fiber and eventually form new fibers themselves.

The development of SCs to eventually form muscle fibers is controlled by a complex interplay of myogenic regulatory factors. Paired box protein 7 (Pax7), is a transcription factor that plays a vital role in regulating myogenic regulatory factors in SCs during early myogenesis (Seale et al., 2000; von Maltzahn et al., 2013). *Pax7* is initially expressed by a pool of myogenic

precursor cells (MPCs) that migrate from the embryonic dermomyotome to the mesoderm during muscle development (Kassar-Duchossoy et al., 2005). Once distributed amongst developing skeletal muscle, the *Pax7* expressing embryonic MPCs undergo differentiation into SCs to establish a quiescent population ready for future myogenesis events (Kassar-Duchossoy et al., 2005).

In response to muscle injury, SCs upregulate the next myogenic regulatory factor, myoblast determination protein 1 (*Myod*), to promote the muscle regeneration process. *Myod* upregulation is considered the step of commitment to differentiation as the produced proteins enhance expression of various skeletal muscle-specific genes to ensure development into myocytes (Davis et al., 1987; Cao et al., 2006). However, not all activated SCs proceed through differentiation as they proliferate through either symmetrical or asymmetrical division. Symmetrical division of activated SCs produces both daughter cells that undergo proliferation or differentiation. Asymmetrical division of an activated SC produces a daughter cell destined for differentiation and another that returns to quiescence (Zammit et al., 2004). Some self-renewing daughter cells continue dividing and eventually decrease *Myod* expression to return to a quiescent state and maintain the SC population. Alternatively, myoblasts destined for terminal differentiation initiate expression of myogenin (*Myog*), a myogenic regulatory factor necessary for fusion into multinucleated myotubes (Adhikari et al., 2021; Tidball, 2017). Expression of *Myog* promotes genes associated with cell cycle exit, further promoting terminal differentiation genes and muscle fiber formation, such as myomaker, a myotube surface fusion protein, and myosin heavy chain (MHC), a structural protein necessary for myofiber contraction (Liu et al., 2012; Wang et al., 2019; Harrison et al., 2011; Luo et al., 2015). Myocyte fusion to form

myotubes can lead to formation of new myofibers or myocytes can fuse with pre-existing damaged muscle fibers for repair (Goh & Millay, 2017).

The expression of *Myog* is regulated in part through histone modifications by methyltransferases. Following embryonic development of muscle tissue, the polycomb repressive complex 2 (PRC2) methyltransferase subunit Ezh2 and regulatory protein Jarid2 methylate histone 3 at lysine 27 (H3K27) to maintain a repressive chromatin state, thus reducing expression of differentiation genes, including *Myog* (Adhikari et al., 2018; Caretti et al., 2004; Wang et al., 2019). In adult skeletal muscle, *Myog* remains transcriptionally silenced because of the association of methyl groups with the histone 3 protein, which facilitates the compact chromosomal structure that conceals the *Myog* locus from transcriptional machinery (Seenundun et al., 2010; Robinson & Dilworth, 2018). Opposing Ezh2 activity, ubiquitously transcribed tetratricopeptide repeat on the X chromosome (Utx), a H3K27me3-specific demethylase, transcriptionally activates some MPC differentiation associated genes (Seenundun et al., 2010). Utx demethylation of H3K27me3 promotes *Myog* expression by loosening the chromosomal structure at the appropriate locus allowing transcription factors access (Bracken et al., 2006; Robinson & Dilworth, 2018). Utx is a well-characterized histone demethylase enzyme specific to H3K27me3 that works to promote differentiation of various pluripotent stem cell types (Xia et al., 2022; Seenundun et al., 2010; Thieme et al., 2013, Tang et al., 2020). However, Utx is not the only histone demethylase specific to H3K27me3.

Jumonji domain containing protein-3 (Jmjd3) is also an H3K27me3 histone demethylase that influences embryonic stem cell differentiation. For example, Jmjd3 can regulate tissue specific cell differentiation in vascular and epidermal tissue (Akiyama et al., 2016; Ohtani et al., 2013; Sen at al., 2008). More recent studies have also shown a significant role for Jmjd3 in

myoblast differentiation during adult skeletal muscle regeneration (Nakka et al., 2022). Although previous investigations described functions for Utx during myogenesis, Jmjd3 has a distinct regulatory role in which it promotes expression of *Has2*, which encodes an extracellular matrix enzyme that allows SCs to receive environmental pro-regenerative signals (Seenundun et al., 2010; Faralli et al., 2016; Nakka et al., 2022).

This investigation looks to further knowledge of the function of Jmjd3 in SCs in vivo. Mice (*Mus musculus*) with hemizygous ablation of Jmjd3 in SCs were studied to determine the effects of reduced *Jmjd3* expression in SCs on the response of muscle to acute injury. The SC specific hemizygous ablation of *Jmjd3* was generated using the Cre recombinase and LoxP flank (Cre-LoxP) system, rather than complete gene knockout due to lethality of complete *Jmjd3* ablation. In this investigation we demonstrate various ways in which changes in *Jmjd3* expression impact regeneration following acute injury.

Materials and Methods

Animals

Animal experimentation was approved by the UCLA Animal Research Committee and complied with established guidelines. Cre-LoxP system was used to develop mice with satellite cell specific hemizygous deletion of Jmjd3. Initial mice were generated by crossing loxP-Jmjd3-loxP$^{+/+}$ mice (Jax Labs, B6.Cg-*Kdm6b*tm1.1Rbo/J) with Pax7/Cre$^{+/+}$ mice (Jaxs Labs, *Pax7*tm1(cre)Mrc/J) to generate loxP-Jmjd3-loxP$^{+/-}$, Pax7/cre$^{+/-}$ hemizygous mice. The hemizygous mice were then backcrossed with loxP-Jmjd3-loxP$^{+/+}$ mice to produce four genotypes: loxP-Jmjd3-loxP$^{+/+}$, Pax7/cre$^{-/-}$ mice (Jmjd3 mutant controls); loxP-Jmjd3-loxP$^{+/+}$, Pax7/cre$^{+/-}$ mice (Jmjd3 mutants); loxP-Jmjd3-loxP$^{+/-}$, Pax7/cre$^{-/-}$ mice (Jmjd3 controls); and loxP-Jmjd3-loxP$^{+/-}$, Pax7/cre$^{+/-}$ mice (Jmjd3 hemizygous mutant). Thirteen Jmjd3 control mice

and 13 Jmjd3 hemizygous mutant mice were bred and cared for in a pathogen-free vivarium at the University of California, Los Angeles.

Tissue Sample Collection & Sectioning

At six months of age, 13 Jmjd3 control and 13 hemizygous mutant mice were injured by BaCl injection to the right hind tibialis anterior muscle. Seven days post-injury (dpi), 6 Jmjd3 control mice and 7 Jmjd3 hemizygous mutant mice were sacrificed by isoflurane inhalation and cervical dislocation, then tibialis anterior muscles were dissected to obtain non-injured and injured muscle tissue samples from both Jmjd3 control and Jmjd3 hemizygous mutant mice at an early stage of injured muscle recovery. After 21-dpi, 7 Jmjd3 control mice and 6 Jmjd3 hemizygous mutant mice were similarly sacrificed and dissected to obtain muscle tissue at a later stage of injured muscle recovery. All muscle samples were immediately weighed, flash frozen in O.C.T. compound, then placed in separate vials containing liquid nitrogen cooled isopentane for storage at -80° C.

Muscle tissue was sectioned to prepare samples for various immunohistochemistry and immunofluorescent staining. Samples in isopentane vials stored at -80° C were transferred into a -20° C freezer for 2 hours to reach optimal cutting temperature. The tibialis anterior muscles were cut in half at the mid-belly, then positioned perpendicular to muscle fiber striation for cross sectioning. Cross sections were cut to 10 μm thickness from the muscle mid-belly towards the origin, then collected on poly-L-lysine coated glass slides. Tissue containing slides were stored at -20° C.

Immunohistochemistry

Cross Sectional Area

Cross sectional area (CSA) measurements were taken to examine overall changes in fiber structure and growth in response to reduced satellite cell Jmjd3 expression and injury. Muscle sections were incubated in 4° C hematoxylin stain for 20 minutes, then rinsed with distilled water. Stained muscle sections were imaged at 20x magnification using a digital imaging software Bioquant, then analyzed using ImageJ to measure muscle fiber CSA. Measurements were performed by manual tracing of 500 random muscle fibers in each tissue sample. Muscle fiber count threshold was determined by increasing the number of fibers counted until no change more than 5% in standard deviation occurred (White et al., 2009). Only regions with central nucleation were measured in the injured tissue samples to capture data from muscle fibers in the process of regeneration (Miller et al., 2000). The average CSA of Jmjd3 control mice was compared to the Jmjd3 hemizygous mutant mice at 7- and 21-dpi to determine changes in fiber growth following acute injury due to the reduction in Jmjd3 expression.

Dystrophin/Hematoxylin Myonuclei Stain

Muscle sections were stained with dystrophin to visualize the fiber membrane, then hematoxylin to highlight the myonuclei within the fiber membrane allowing for the changes in myonuclei count in response to reduced SC *Jmjd3* expression and injury. Sections were first air dried for 30 minutes at room temperature before being fixed with -20° C acetone for 10 minutes. Muscle sections were next submerged in 0.3% hydrogen peroxide to block horseradish peroxidase from binding non-specifically to endogenous peroxidases. Muscle sections were also incubated with a mouse-on-mouse (M.O.M.) block reagent, followed by M.O.M. protein diluent (Vector Laboratories, Cat. # PK-2200) to block mouse immunoglobulin from endogenously binding mouse antibody. Next, the muscle sections were incubated with anti-dystrophin stain (Novocastra, Cat. #NCL-DYS2, Lot #6067485, 1:30) overnight at 4º C. The avidin-biotin

complex detection method was used to react with the anti-dystrophin primary antibody (Bratthauer, 2010). Biotinylated anti-mouse secondary antibody followed by a time-critical AEC development step (Abcam, Cat. #ab64252) was added to the muscle sections producing a red reaction product to illuminate the fiber membrane. Finally, the muscle sections were incubated in 4° C hematoxylin for 20 minutes to stain the nucleic acid rich myonuclei.

The myonuclei were quantified using an Olympus BH50 microscope at 40x magnification. The number of hematoxylin-stained central nuclei within the dystrophin-stained membranes of 500 muscle fibers were quantified to determine amounts of actively regenerating fibers in non-injured or injured muscle (Bigard et al., 1997). The areas in and around the afflicted site of injured muscle sections were counted to acquire injury specific data.

Immunofluorescence

Fluorescent antibody staining was performed on muscle sections to investigate changes in satellite cell protein expression during myogenesis in response to reduced SC *Jmjd3* expression and injury. Muscle sections were labeled with Pax7 to identify SCs, then another antibody to determine the presence of proteins of interest, and finally DAPI to visualize cell nuclei. Muscle sections were thawed to 20° C for 30 minutes, then incubated in 4% paraformaldehyde to fix proteins. Sections were next washed in phosphate buffered saline (PBS) before being immersed for 40 minutes in 95° C sodium citrate buffer containing 0.05% Tween-20 (pH 6.0) to expose antigens for staining with primary antibodies. Next, muscle sections were incubated with a M.O.M. block reagent, followed by M.O.M. protein diluent (Vector Laboratories, Cat. # PK-2200). Sections were then co-labeled overnight in a humidified chamber at 4° C with anti-Pax7 (SCBT, Cat. #sc-81648, 1:20) and either anti-H3K27me3 (CST, Cat. #9733, 1:1500) or anti-Ki67 (Invitrogen, Cat. #14-5698-82). Conjugated fluorescent secondary antibodies, anti-mouse IgG on

DyLight 594 (Vector Labs, Cat. #DI-2594, 1:100) and anti-rabbit IgG on DyLight 488 (Vector Labs, Cat. #DI-1088, 1:100), were used to illuminate the primary antibodies. Muscle sections were mounted with Prolong Gold Antifade Mountant containing DAPI DNA stain (Invitrogen, Cat. #P36931). Data were collected as a percent of double positive SCs out of total $Pax7^+$ cells. SCs were identified by their position at the muscle fiber periphery, beneath or just outside the basal lamina, and by the presence of both Pax7 and DAPI DNA fluorescence. SCs were considered positive for the other immunolabeled marker of interest based on overlap with Pax7 and DAPI fluorescence suggesting double positive cells containing both the marker of interest and Pax7 labelling.

In vitro RNA

C2C12 Culture Treatment

Immortalized mouse myoblast C2C12 cells were used for in vitro treatment (Blau et al., 1985). Myoblasts were seeded at 200,000 cells per 10 cm culture plate and maintained in growth medium (Dulbecco's Modified Eagle Medium (DMEM) containing 1% penicillin/streptomycin, and 10% fetal bovine serum (FBS)) at 37°C with 5% CO_2. Growth medium was changed every 48 hours to replenish nutrients and remove metabolite waste. For myoblast treatment, cells were grown to confluence, then the medium was changed to differentiation medium (DMEM containing 1% penicillin/streptomycin) for 24 hours to initiate myotube formation. Following 24 hours with differentiation medium, the 10% FBS growth medium was reintroduced to the cells to promote myotube formation and eventual fusion for myofiber formation.

Quantitative PCR of developing C2C12 treated with GSK-J4

A pharmacological inhibitor targeting H3K27 demethylases, called GSK-J4, was used in treating C2C12 cells to mimic the differentiation of SCs following acute injury in the mice bred

with satellite cell-specific Jmjd3 hemizygous expression. C2C12 cells were treated with 2 μM GSK-J4 (Millipore Sigma, Cat. # SML0701) or vehicle control for 48 hours prior to RNA collection at 70% confluence ($C2C12^{70}$), 1-day post-starvation ($C2C12^{1\text{-day}}$), and 4-days post-starvation ($C2C12^{4\text{-day}}$) to examine C2C12 cells at various stages of myogenesis with inhibition of Jmjd3 demethylase activity at the H3K27 locus. At each collection time point cells were washed of growth media proteins, homogenized with Trizol (Invitrogen, Cat. #15596026), and RNA was extracted with chloroform, then precipitated with isopropanol. After the RNA was collected, it was next DNase-treated and purified with a RNeasy Mini Kit (Qiagen, Cat. #74106) to avoid degradation and eliminate contamination. The RNA concentration was quantified using a spectrophotometer (Beckman, Cat. #DU730) at 260 nm absorbance to allow for RNA concentration to be normalized across samples. RNA quality was determined by electrophoresis to visualize clear separation between 28S and 18S ribosomal RNA, while concentration was evaluated based on RNA band intensity. RNA samples were stored at -20° C between extraction, purification, reverse transcription, and PCR analysis.

Purified RNA samples were reverse transcribed in 2 μg aliquots with Super Script Reverse Transcriptase II (Invitrogen, Cat. #18064071) using Oligo-dT Primers (Invitrogen, Cat. # AM5730G) for construction of cDNA of interest (Table 1). The generated cDNA was used with SYBR Green qPCR Master Mix (Bio-Rad, Cat. #1725150) to run RT-qPCR on an iQ5 thermocycler (Bio-Rad, Cat. #170-9780) with optical system software (Bio-Rad, Cat. #170-9753SE01). *Hagh* and *Tbp* were used as reference genes. The geometric means of Ct-values from the reference genes were used to calculate the normalization factor for each sample, then the highest relative expression values for each gene were set to a factor of 1 and the others were scaled equally.

Gene	Forward	Reverse
Myog	CCAGTACATTGAGCGCCTAC	ACCGACTCCAGTGCATTGC
Myomaker	CGTAGGTGTAATCCCATTCCTCA	CGTAGGTGTAATCCCATTCCTCA
Pax7	CTCAGTGAGTTCGATTAGCCG	AGACGGTTCCCTTTGTCGC
Shisa2	GCTGCGCTACTGCTGCTCC	GAACACTGAGCCAACGATGAG
Hagh	CACCACTCACCACCACTGG	ACACTGAGAGACCCCACCTG
Tbp	TCCCCCTCTGCACTGAAATC	AGTGCCGCCCAAGTAGCA

Table 1. Sequences of primers used for reverse transcription to generate cDNA.

Statistics

The mean ± standard error of the mean (SEM) was used to graphically represent the data. Differences between two groups were determined by multiple nonparametric t-tests, while differences between multiple groups and a control group were determined by one-way analysis of variance (one-way ANOVA). Significant difference was determined in group comparisons with $p < 0.05$.

Results

Jmjd3 decreased di- and trimethylated H3K27 at 7- and 21-dpi

The demethylation of H3K27 in differentiating SCs has previously been reported to play a crucial role in regulating myogenic factor gene expression (Faralli et al., 2016). To investigate the impact of reduced SC *Jmjd3* expression in the Jmjd3 hemizygous mutant mice on SC behavior and epigenetic modifications following muscle injury, we performed immunofluorescent staining and quantification of H3K27me2/3^{+}Pax7^{+} cells out of total Pax7^{+} cells at 7- and 21-dpi.

At 7-dpi, the injured Jmjd3 hemizygous mutant mice had a 40% greater proportion of Pax7^{+} cells that were H3K27me2/3^{+} compared to the injured Jmjd3 controls ($p = 0.041$) (Figure 1a; Figure 1b; Supp. Figure 1). Similarly, the 21-dpi injured Jmjd3 hemizygous mutant mice had ~100% greater proportion of Pax7^{+} cells that were H3K27me2/3^{+}/Pax7^{+} compared to the 21-dpi

injured Jmjd3 controls ($p = 0.0003$) (Figure 1a; Figure 1b; Supp. Figure 1). Interestingly, at 7-dpi the SCs of non-injured mice also showed significant difference in proportion of $Pax7^+$ cells expressing H3K27me2/3$^+$/$Pax7^+$ when comparing the Jmjd3 controls to Jmjd3 hemizygous mutant mice ($p = 0.0004$) (Figure 1a; Figure 1b; Supp. Figure 1). However, at 21-dpi the SCs of non-injured mice did not show significant difference in proportion of $Pax7^+$ cells expressing H3K27me2/3$^+$/$Pax7^+$ when comparing the Jmjd3 controls to Jmjd3 hemizygous mutant mice. These results indicate that the SCs of Jmjd3 hemizygous mutant mice contain reduced Jmjd3 demethylase activity compared to the Jmjd3 control mice, and therefore a higher proportion of SCs remain H3K27me2/3$^+$.

We further investigated the effects of reduced *Jmjd3* expression by examining C2C12 cells treated with GSK-J4, an H3K27 demethylase inhibitory drug. The C2C12 cells treated with GSK-J4 are used as the *in vitro* model for Jmjd3 hemizygous mutant mice because the drug inhibits histone demethylase activity including Jmjd3 activity at H3K27me3. The GSK-J4 treated C2C12 cells had higher *Myog* RNA expression at 70% confluence ($p = 0.028$), no effect on *Myog* RNA expression at 1-day post-differentiation medium, and again higher expression at 4-days post-differentiation medium ($p = 0.014$) when compared to control (Figure 1c). At 70% confluence the *Myog* expression in GSK-J4 treated cells is 189.8% higher than controls, and 36.54% higher than controls at 4-days post-differentiation medium (Figure 1c). The increase of *Myog* expression in C2C12 cells treated with GSK-J4 demethylase inhibitor at 70% confluence and 4-days post-differentiation medium may suggest that other histone demethylases are available to promote a more permissive chromatin structure for *Myog* expression.

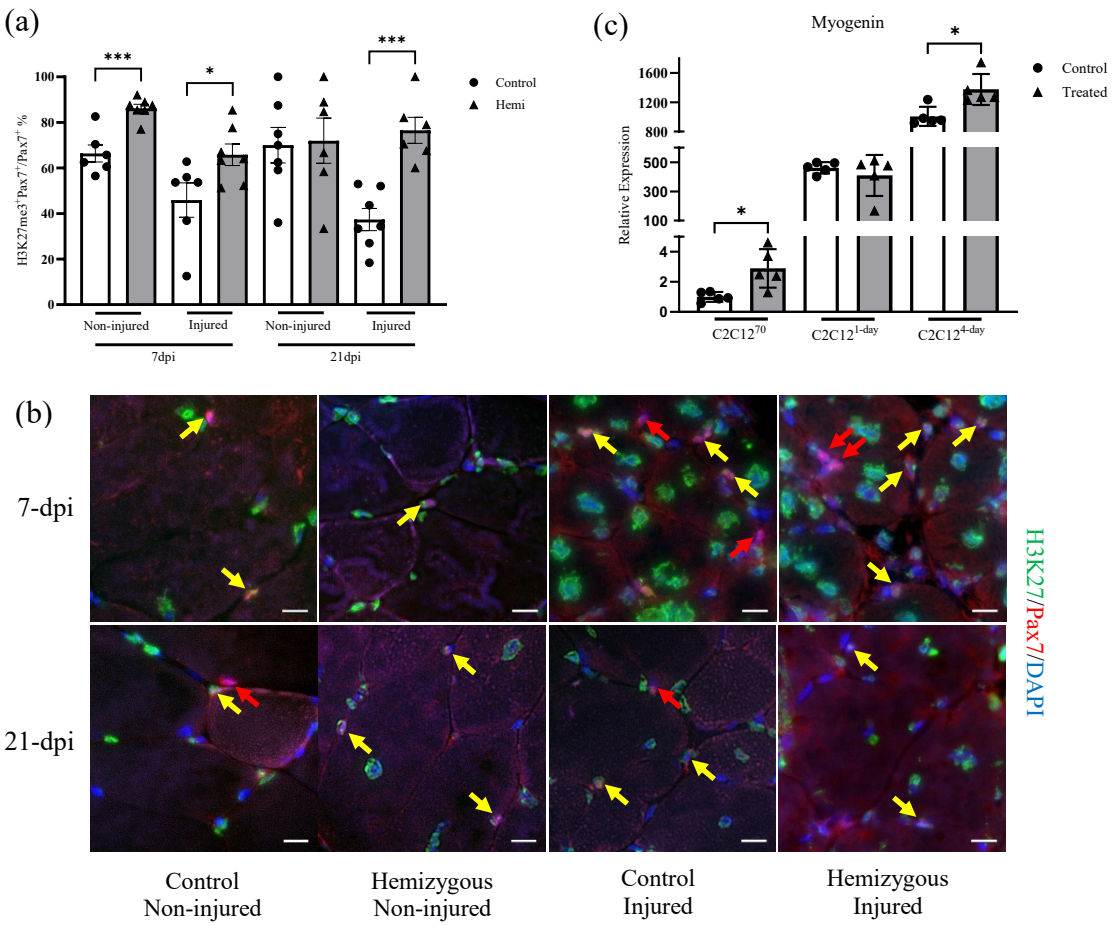

*Figure 1. Mutation of Jmjd3 in SCs affects demethylation of H3K27me2/3. (a) Ratio of H3K27me2/3$^+$/Pax7$^+$ cells to total Pax7$^+$ cells in muscle sections of injured Jmjd3 control and mutant mice TA cross-sections at 7- and 21-dpi. The bar plot includes the average percent of H3K27me2/3$^+$ cells out of total Pax7$^+$ cells at the muscle fiber periphery per treatment group (bars) ± SEM, and individual percent H3K27me2/3$^+$/Pax7$^+$ cells per treatment group (points). (b) Representative images of Jmjd3 control and mutant TA muscle at 7- and 21-dpi immunolabeled for H3K27me2/3 (green), Pax7 (red), and DNA labeled with DAPI (blue). The yellow arrows indicate H3K27me2/3$^+$/Pax7$^+$ cells and red arrows indicate Pax7$^+$ cells. Scale bars = 20 µm. (c) QPCR data showing relative expression of Myog by C2C12 cells treated with GSK-J4 or with vehicle control for 24 hours of C2C12^{70}, C2C12$^{1\text{-}day}$, and C2C12$^{4\text{-}day}$ cells. The bar plot shows relative expression (bars) ± SEM, with corrected Ct values (points). * $p < 0.05$, *** $p < 001$.*

Jmjd3 hemizygous mutation slows muscle fiber growth

Histone demethylation by Utx at H3K27me2/3 is necessary for efficient muscle fiber growth following acute injury (Faralli et al., 2016; Nakka et al., 2022). We investigated whether the demethylase activity of Jmjd3 similarly promoted muscle fiber growth by comparing the CSA of muscle fibers of Jmjd3 control and Jmjd3 hemizygous mutant mice. At 7-dpi, muscle fiber CSA did not differ between Jmjd3 control and Jmjd3 hemizygous mutant mice. However, non-injured muscle fibers were larger than injured muscle fibers by 31.06% in Jmjd3 control mice ($p = 0.0008$) and 29.56% in Jmjd3 hemizygous mutant mice ($p = 2.9 \times 10^{-5}$) (Figure 2a; Figure 2b; Supp. Figure 2). At 21-dpi, muscle fiber CSA in injured Jmjd3 control mice increased to the size of non-injured Jmjd3 control muscle fibers (Figure 2a; Figure 2b; Supp. Figure 2). However, the CSA of fibers in injured Jmjd3 hemizygous mutant muscles were 16.64% smaller than muscle fibers of injured Jmjd3 control mice ($p = 0.016$) (Figure 2a; Figure 2b; Supp. Figure 2). The smaller CSA in Jmjd3 hemizygous mutant mice demonstrates slower muscle fiber growth following injury than occurred in Jmjd3 control mice.

During the later stages of myogenesis, muscle cell fusion contributes to muscle fiber growth as myogenic cells fuse with damaged, pre-existing fibers. Because Shisa2 regulates muscle cell fusion to repair muscle fibers following acute injury (Lui et al., 2018; Wang et al., 2019), we tested whether decreasing H3K27 demethylase activity with GSK-J4 affected *Shisa2* expression. The expression of *Shisa2* was significantly reduced in the GSK-J4 treated C2C12 cells that were assayed after 1 day of growth in differentiation medium ($p = 0.01$) (Figure 2c). However, after 4 days growth in differentiation medium *Shisa2* expression increased in GSK-J4 treated C2C12 cells ($p = 0.014$) (Figure 2c). The effect of GSK-J4 on *Shisa2* expression that

occurred after 1-day in differentiation medium aligned with the decrease in CSA for Jmjd3 hemizygous mutant mice muscle fibers compared to Jmjd3 controls.

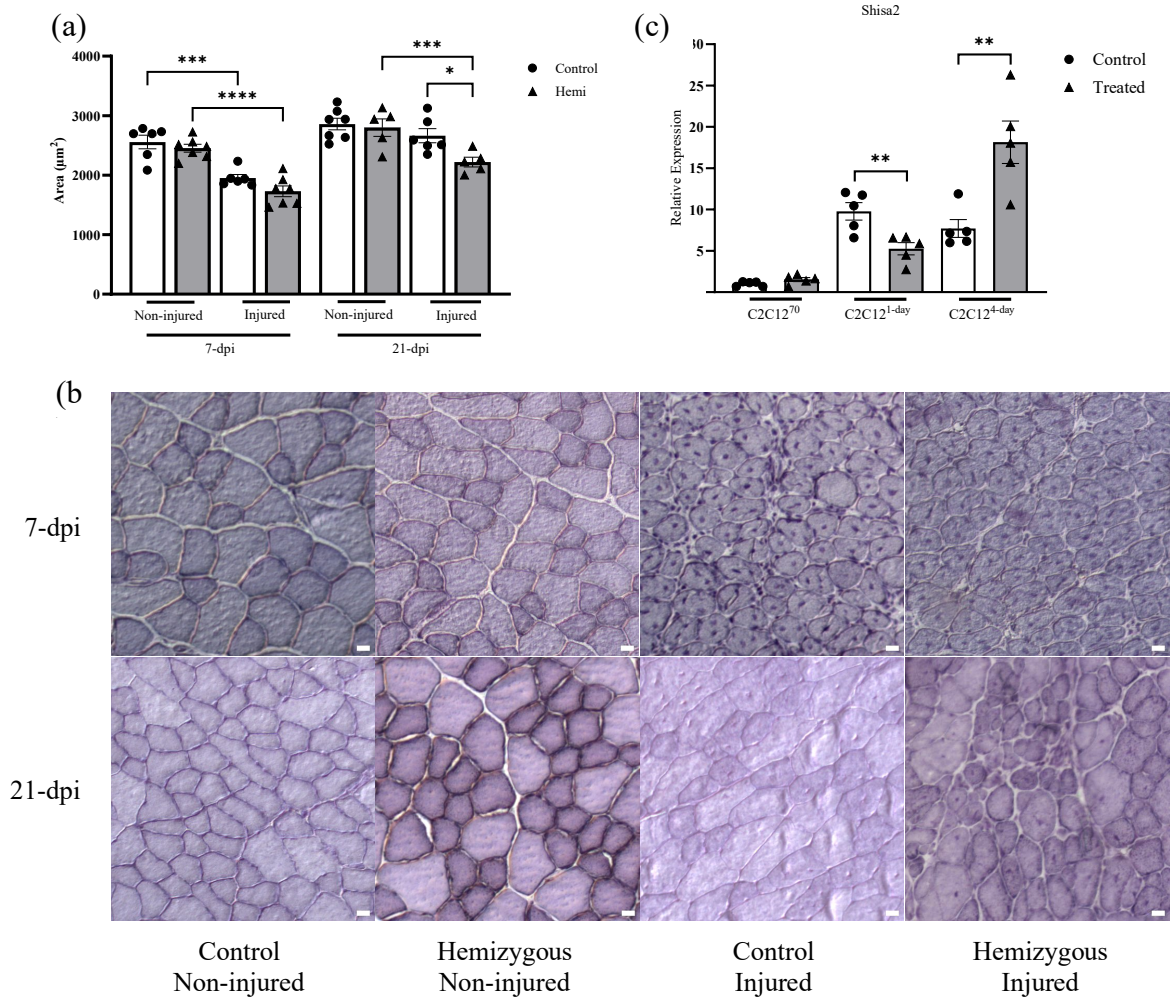

*Figure 2. Mutation of Jmjd3 in SCs affects muscle fiber CSA following acute injury. (a) Muscle fiber CSA of non-injured and injured Jmjd3 control and mutant mice TA cross-sections at 7-dpi and 21-dpi. The bar plot includes average muscle section CSA (bars) ± SEM, with individual CSA measurements (μm^2) per treatment group (points). (b) Representative images of non-injured and injured Jmjd3 control and mutant TA muscle at 7- and 21-dpi stained with hematoxylin. Scale bars = 20 µm. (c) QPCR data showing relative expression of Shisa2 from in vitro C2C12 cells when treated with GSK-J4, or with vehicle control, for 24 hours of $C2C12^{70}$, $C2C12^{1\text{-}day}$, and $C2C12^{4\text{-}day}$ cells. The bar plot shows average relative expression (bars) ± SEM, with corrected Ct values (points). * $p < 0.05$, ** $p < 0.01$.*

Jmjd3 hemizygous mutation does not influence the number of myonuclei per muscle fiber during muscle repair following injury

Muscle fiber repair following injury can involve myogenic cells that fuse with damaged muscle fibers creating larger fibers and increasing the number of myonuclei per fiber (Adhikari et al., 2021). Because the CSA of muscle fibers in injured Jmjd3 hemizygous mutant mice was less than Jmjd3 control mice at 21-dpi, we examined the effects of reduced *Jmjd3* expression on the number of myonuclei per muscle fiber.

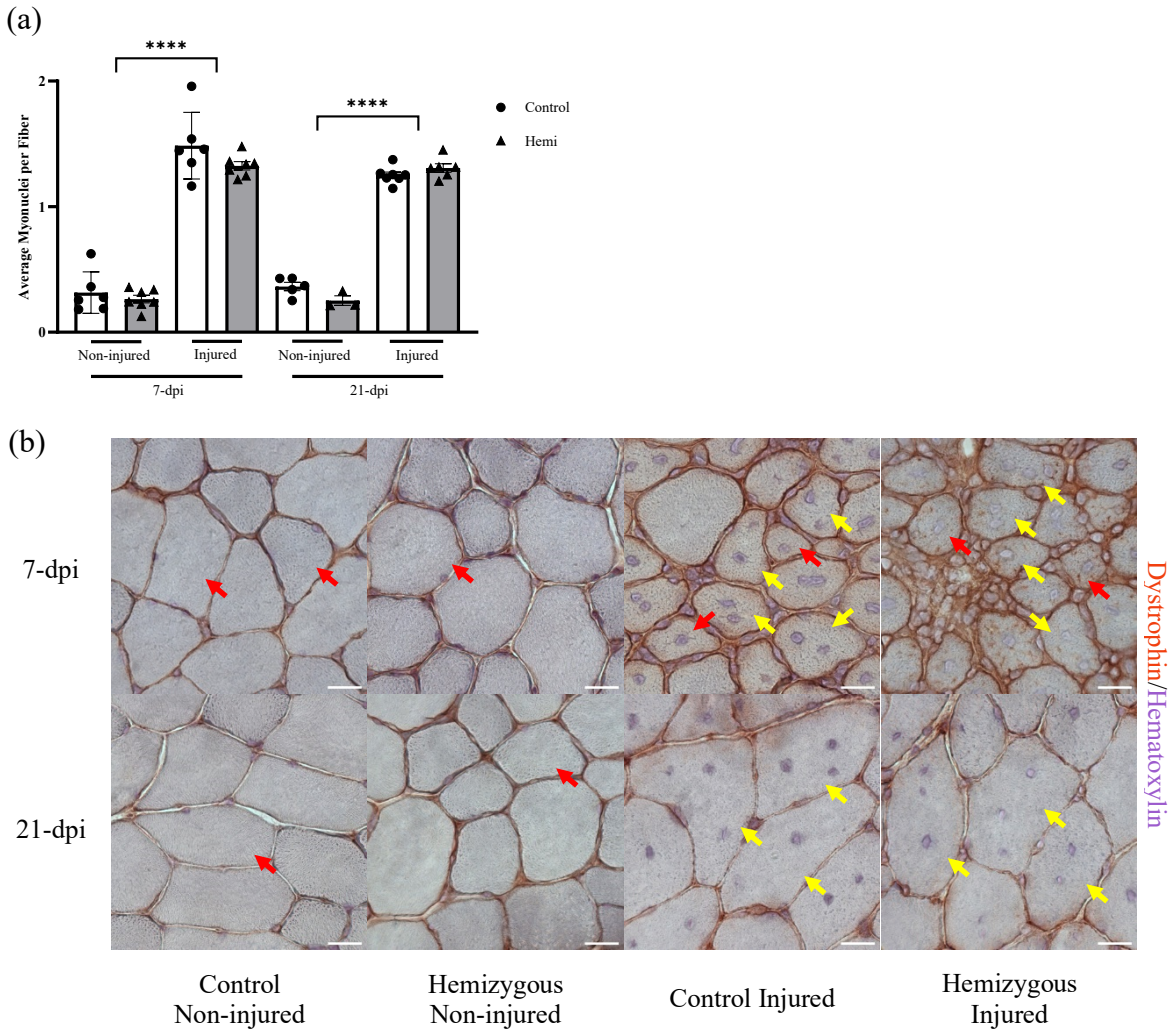

Figure 3. Injury to TA muscle tissue affects number of myonuclei. Jmjd3 hemizygous mutation in SCs is not associated with significant changes in myonuclei number per muscle muscle fiber. (a) Number of myonuclei per 500 fibers in TA from non-injured and injured Jmjd3 control and mutant mice TA cross-

*sections at 7-dpi and 21-dpi. The bar graph shows average myonuclei per 500 fibers in all treatment groups ± SEM, and individual myonuclei per 500 fibers in all treatment groups. **** $p < 0.0001$. (b) Representative images of non-injured and injured Jmjd3 control and mutant TA muscle at 7-dpi and 21-dpi immunolabeled for dystrophin (reddish-brown membrane) and hematoxylin (purple nuclei). Red arrows indicate muscle fibers with one nuclei and yellow arrows indicate muscle fibers with multiple nuclei. Scale bars = 20 µm.*

A comparison of myonuclei per muscle fiber in Jmjd3 hemizygous mutant mice muscle and Jmjd3 control mice revealed no significant difference between the two genotypes. However, there was a significant difference of injured muscle containing more myonuclei per muscle fiber than non-injured muscle ($p < 0.0001$) (Figure 3a; Figure 3b). The difference in only non-injured compared to injured muscle sections suggests that the reduced *Jmjd3* expression did not change myonuclei count per muscle fiber, but injury had a positive influence on the number of myonuclei.

Jmjd3 hemizygous mutation increases satellite cell proliferation during myogenesis

Expression of *Ki67* in SCs indicates their activation and proliferation (Guitart et al., 2017; Mackey et al., 2009; Fry et al., 2016; Wehling-Henricks et al., 2016). To determine whether SCs are maintained in a proliferative state when *Jmjd3* expression is reduced, we examined whether there were changes to the proportion of SCs expressing Ki67.

Our findings show that the proportion of SCs in injured muscles that express detectible Ki67 was decreased by Jmjd3 mutation. The proportion of SCs in injured muscles of Jmjd3 hemizygous mutant mice that were $Ki67^+$ was 22.89% less than in the injured Jmjd3 control mice at 7-dpi ($p = 0.0018$) (Figure 4a; Figure 4b; Supp. Figure 3). Similarly, at 21-dpi, the injured Jmjd3 hemizygous mutant mice muscle sections had a significantly smaller proportion of SCs that were

Ki67$^+$ than the injured Jmjd3 control mice muscle sections (p = 0.003) (Figure 4; Figure 4b; Supp. Figure 3).

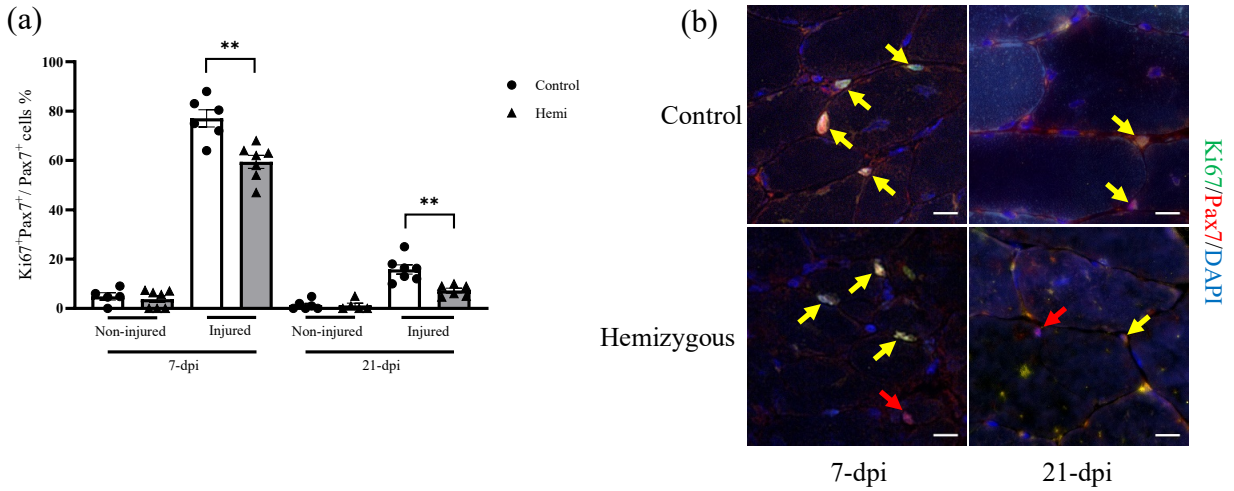

*Figure 4. Mutation of Jmjd3 in SCs affects proliferation following acute injury. (a) Ratio of Ki67$^+$Pax7$^+$ cells to total Pax7$^+$ cells in muscle sections of non-injured and injured Jmjd3 control and Jmjd3 hemizygous mutant mice TA at 7- and 21-dpi. The bar plot shows average Ki67$^+$Pax7$^+$ cells out of total Pax7$^+$ cells at the muscle fiber periphery per treatment group (bars) ± SEM, and individual percent Ki67$^+$Pax7$^+$/Pax7$^+$ cell counts per treatment group (points). ** p < 0.005. (b) Representative images of Jmjd3 control and mutant TA muscle at 7- and 21-dpi immunolabeled for Ki67 (green), Pax7 (red), and DNA labeled with DAPI (blue). The yellow arrows indicate Ki67$^+$/Pax7$^+$ cell and red arrows indicate Pax7$^+$ cell. Scale bars = 20 μm.*

Discussion

The current investigation demonstrates that hemizygous mutation of Jmjd3 influences adult skeletal muscle regeneration following acute injury. Our findings show the proportion of H3K27me2/3$^+$/Pax7$^+$ cells out of total Pax7$^+$ cells increased in acutely injured Jmjd3 hemizygous mutant mice, suggesting that the mutation reduced H3K27me2/3 demethylation. We also found that Jmjd3 mutation reduced the average cross-sectional area of muscle fibers following muscle injury but did not significantly affect the number of myonuclei per muscle fiber. In addition, the

Jmjd3 hemizygous mutation reduced the proportion of SCs that were proliferating in injured muscle when compared to Jmjd3 control mice. *In vitro*, *Shisa2* expression was decreased by H3K27 demethylase inhibition at some stages of C2C12 differentiation *in vitro*, but increased at other stages, suggesting that the influence of H3K27 demethylation on muscle cell fusion may vary with the stage of myogenesis.

The reduced proportion of H3K27me2/3^{+}/Pax7^{+} cells out of total Pax7^{+} cells following acute injury to Jmjd3 hemizygous mutant muscle compared to control mice is interesting because previous literature showed the importance of H3K27me3 demethylation for activation of SC differentiation genes (Wang et al., 2019). Culturing porcine SCs to various stages of differentiation revealed that H3K27 methylation obstructs expression of myogenic transcription factors by modifying the chromatin state (Wang et al., 2019). Wang et al. observed a 50% reduction of H3K27me3 marks in differentiating SCs compared to proliferating SCs (Wang et al., 2019). The reduction of H3K27me3 methyl marks increased SC exit from the cell cycle and initiated cell differentiation, allowing upregulation of differentiation genes like *Myog*.

Although we did not assay changes in myogenic regulatory gene expression caused by the Jmjd3 mutation in SCs *in vivo,* our *in vitro* expression analysis of C2C12 cells treated with GSK-J4 showed changes to *Myog* expression. We found that the GSK-J4 treatment, and presumed reduction in H3K27me3 demethylation, led to an increase in *Myog* transcripts, suggesting the promotion of differentiation into myocytes. However, our results apparently contrast with the findings of previous investigators (Wang et al., 2019; McKee et al., 2022; Nakka et al., 2022). McKee et al. (2022) downregulated Jmjd3 by treating myoblasts with Jmjd3 siRNA and found a 50% reduction in *Myog* transcripts. In addition, upregulating Jmjd3 by transfecting myoblasts with a *Jmjd3* expression plasmid produced a nearly 100% increase in

Myog expression (McKee et al., 2022). Those findings indicate a positive relationship between Jmjd3 and *Myog* expression (McKee et al., 2022). Similarly, porcine SCs cultured by Wang et al. (2019) possessed highly myogenic differentiation potential at 2-days of differentiation (D2) compared to proliferating cells indicated by differentiation marker myogenin, myotube formation, and myofiber establishment. The D2 cells were previously demonstrated to contain reduced H3K27me3 methyl marks as histone demethylation increased to promote upregulation of differentiation genes, thus suggesting a positive relationship with histone demethylase Jmjd3 (Wang et al., 2019). Both McKee et al. and Wang et al. demonstrate positive relationships between Jmjd3 histone demethylase activity and *Myog* expression contrary to our results. However, other investigators examined muscle of mice with tamoxifen-inducible SC-specific knockout of Jmjd3 ($Jmjd3^{scKO}$) at 30 hours after cardiotoxin injection and found no statistically significant change in *myogenin* expression (Nakka et al., 2022). The variations in the relationship between Jmjd3 and *Myog* expression may be due to differing levels of Jmjd3 reduction resulting in variable changes to *Myog* expression. In addition, our findings may differ from the results of investigations that studied the effects of increased or decreased *Jmjd3* expression because we used a non-specific H3K27 demethylase inhibitor. Treating C2C12 cells with GSK-J4 inhibits both Utx and Jmjd3 histone demethylases.

The reduced expression in Jmjd3 hemizygous mutant mice correlated with a reduction in muscle fiber CSA, indicating a positive relationship between *Jmjd3* expression and muscle fiber growth following injury. Although fiber CSA did not differ significantly between hemizygous mutant and control mice muscle at 7-dpi, the injured mutant mice muscle at 21-dpi had significantly reduced fiber CSA compared to control suggesting an inhibition of muscle fiber growth. The decrease in CSA with reduced *Jmjd3* expression following acute injury was also

seen in previous literature aimed to determine whether Utx and Jmjd3 had compensatory roles in fiber growth following acute injury (Nakka et al., 2022). Nakka et al. observed a significant decrease in CSA in both JMJD3^{scKO} and UTX^{scKO} injured muscle compared to wild-type at 7-dpi, which contrasts with our findings. However, the stronger treatment effect reported by Nakka et al. at 7-dpi may reflect that in their model both Jmjd3 alleles were targeted, unlike our hemizygous model.

The changes in muscle fiber growth demonstrated by reduced fiber CSA led us to further investigate the effects of reduced *Jmjd3* expression on myocyte fusion. We explored the link between reduced *Jmdj3* expression and myocyte fusion by examining the number of myonuclei per muscle fiber but found no difference between Jmjd3 hemizygous mutant and control mice at either 7- or 21-dpi. Our *in vivo* findings are consistent with previous *in vitro* findings which showed that Jmjd3 mutation in myogenic cells did not affect fusion efficiency, the percent of nuclei present in multinucleated myotubes, or fusion index, the mean number of nuclei per myosin heavy chain positive myofiber (Nakka et al., 2022). Interestingly, the same investigators found reductions of fusion efficiency and fusion index in UTX^{scKO} mice, suggesting Utx is necessary for terminal muscle differentiation rather than Jmjd3 (Nakka et al., 2022). Although Jmjd3 mutation did not affect muscle cell fusion *in vivo* or *in vitro* (Nakka et al., 2022; present investigation), reduction in *Jmjd3* expression can increase expression of *Shisa2* (Nakka et al., 2022), a protein that promotes fusion (Lui et al., 2018). Previous studies investigated the role of Shisa2 in myoblast fusion during differentiation by examining differentiating myocytes infected with *Shisa2* overexpression (OE) adenovirus following acute injury (Lui et al., 2018). They observed a significant increase in the percentage of myotubes containing over 10 myonuclei compared to controls suggesting *Shisa2* expression promotes myocyte fusion during the

formation of myotubes (Lui et al., 2018). Although *Shisa2* expression in SCs isolated from muscle 30 hours after cardiotoxin injection was increased significantly by Jmjd3 mutation (Nakka et al., 2022), the investigators did not observe an influence of the mutation on fusion. A possible reason for the lack of increased myonuclei per muscle fiber may be the increase in expression of *Shisa2* was much less than the 200-fold increase in Shisa2 OE myocytes (Lui et al., 2018).

Our finding that the proportion of $Ki67^{+}/Pax7^{+}$ SCs in Jmjd3 hemizygous mutant mice was less than in controls indicates that Jmjd3 promotes SC proliferation. This is consistent with previous findings that SC incorporation of 5-ethynyl-2'-deoxyuridine (EdU) to identify cells undergoing DNA replication was significantly less in $JMJD3^{scKO}$ mice, indicating reduced proliferation (Nakka et al., 2022). Furthermore, our data suggesting SC proliferation is reduced in Jmjd3 hemizygous mutant mice with impaired muscle growth is supported by previous literature connecting SC proliferation to a similar myogenic outcome (Wen et al., 2012). When analyzing myoblasts overexpressing Notch1, a regulator of satellite cell fate, the number of $Ki67^{+}$ cells decreased to less than half compared to controls. This reduction was greater than the decrease of $Ki67^{+}/Pax7^{+}$ SCs observed in our Jmjd3 hemizygous mutant mice compared to controls (Wen et al., 2012). Interestingly, Wen et al. also found increased $Pax7^{+}$ expression in myoblasts and were able to determine the increase was not a secondary effect from MyoD or myogenin inhibition by examining overexpression of various Notch1 targets (Wen et al., 2012). As our data focus on the proportion of $Ki67^{+}/Pax7^{+}$ out of total $Pax7^{+}$ cells, further investigation of whether the reduced proportion of $Ki67^{+}/Pax7^{+}$ SCs is due to increased total $Pax7^{+}$ cells rather than a reduction of double positive cells would help assess the changes to SC proliferation.

In conclusion, the present study shows that decreased *Jmjd3* expression in Jmjd3 hemizygous mutant mice reduced the proportion of SCs that were proliferating, which was associated with slower muscle fiber growth following injury. Despite a similar H3K27me2/3 demethylase role by Utx in SCs (Seenundun et al., 2010), our data demonstrate that Jmjd3 downregulation is sufficient to attenuate H2K27 demethylase activity during myogenesis. Although changes in expression of *myogenin* and *Shisa2* occurred in myogenic cells treated with non-specific H3K27 demethylases inhibitor, a Jmjd3-specific inhibitor would be necessary to ensure the results were due to Jmjd3 and not Utx. Further investigation into *Jmjd3* expression during myogenesis may reveal a more in-depth understanding of its histone demethylase role at pivotal steps throughout muscle regeneration.

Supplementary Data

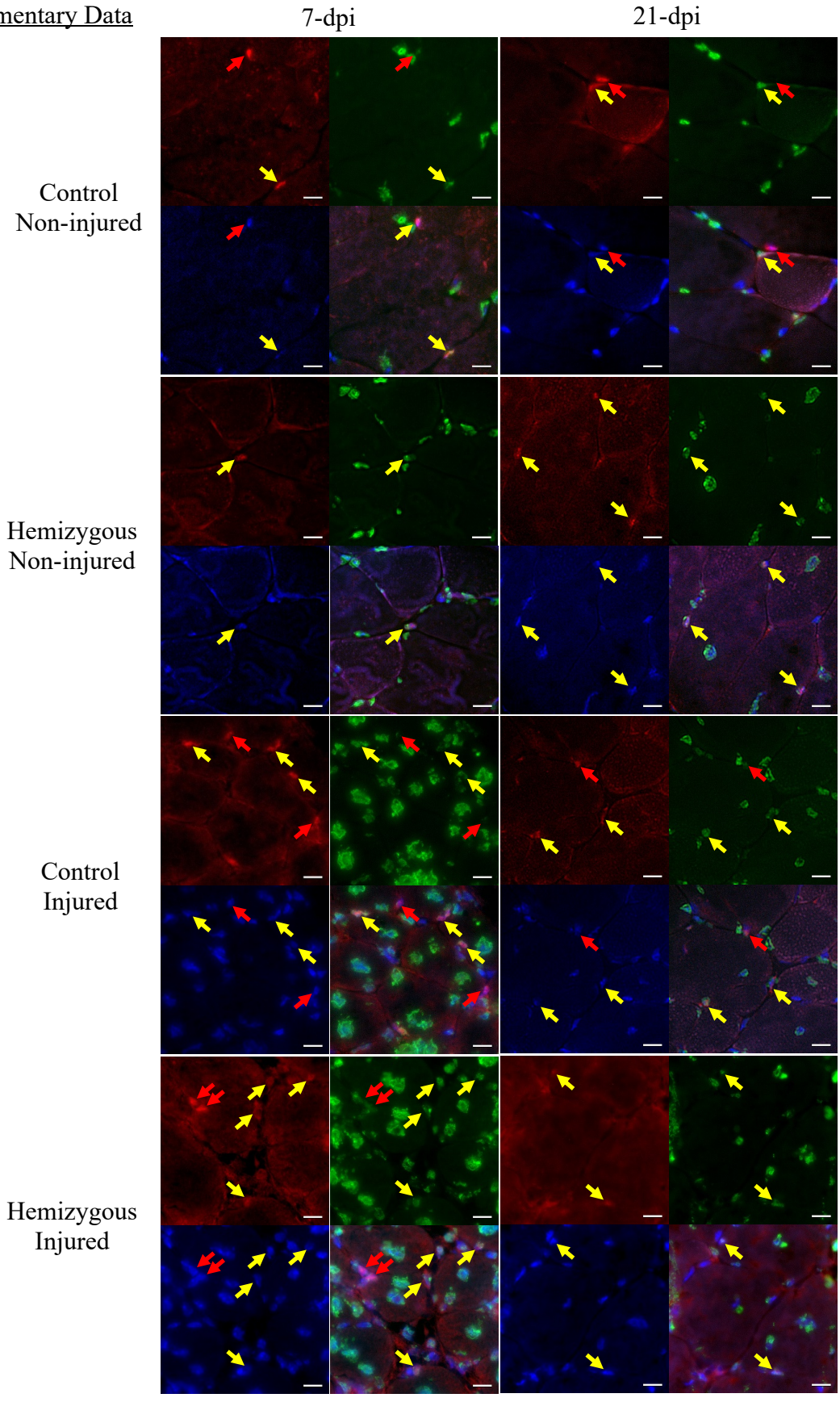

Supplementary Figure 1. Mutation of Jmjd3 in SCs affects demethylation of H3K27me2/3. Representative images of Jmjd3 control and mutant TA muscle at 7- and 21-dpi immunolabeled for H3K27me2/3 (green), Pax7 (red), and DNA labeled with DAPI (blue). The yellow arrows indicate H3K27me2/3^{+}/Pax7^{+} cells and red arrows indicate Pax7^{+} cells. Scale bars = 20 μm.

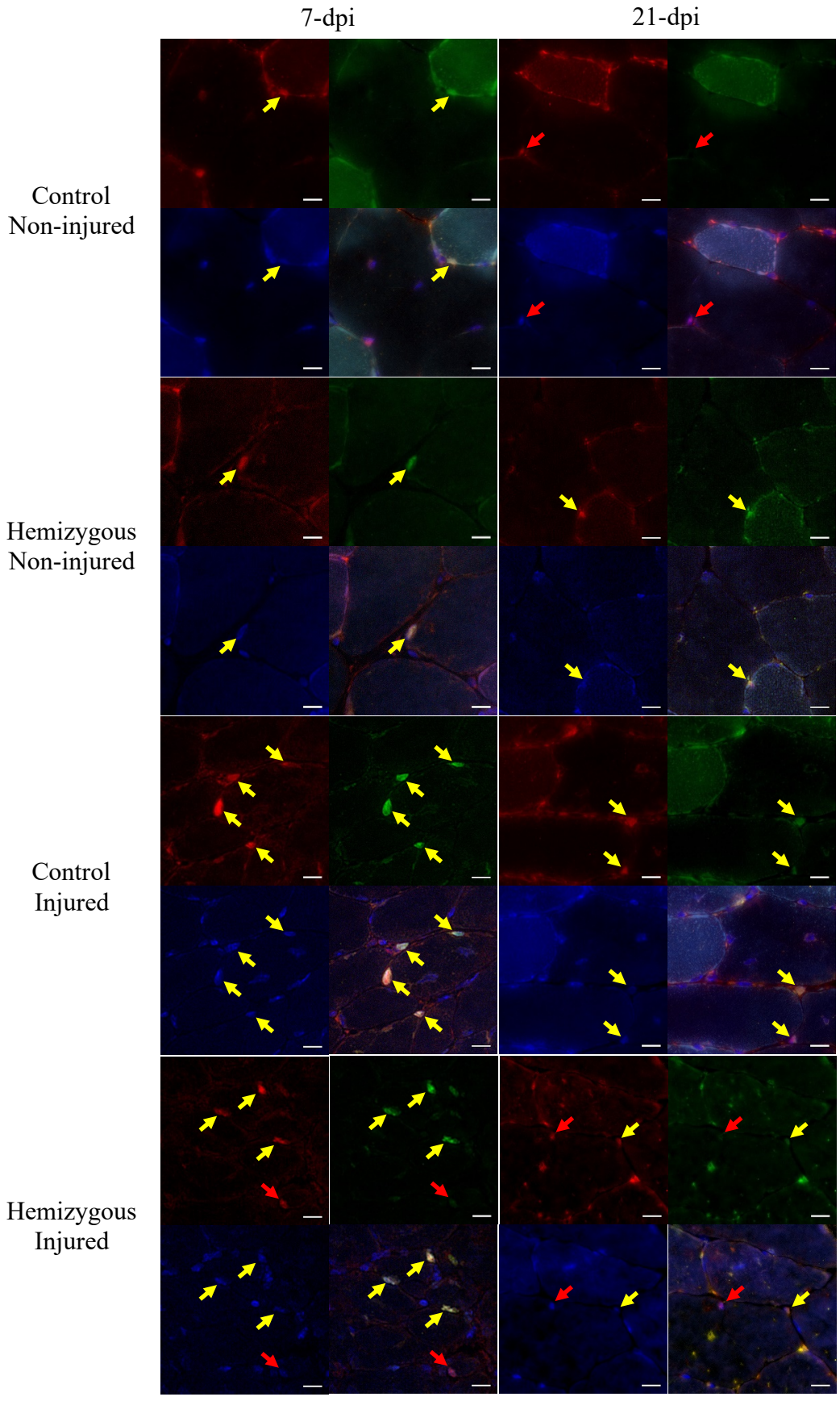
7-dpi
21-dpi
Control
Non-injured
Hemizygous
Non-injured
Control
Injured
Hemizygous
Injured

Supplementary Figure 2. Mutation of Jmjd3 in SCs affects proliferation. Representative images of Jmjd3 control and mutant TA muscle at 7- and 21-dpi immunolabeled for Ki67 (green), Pax7 (red), and DNA labeled with DAPI (blue). The yellow arrows indicate $Ki67^{+}/Pax7^{+}$ cells and red arrows indicate $Pax7^{+}$ cell. Scale bars = 20 μm.

References

Adhikari, A., & Davie, J. (2018). JARID2 and the PRC2 complex regulate skeletal muscle differentiation through regulation of canonical Wnt signaling. *Epigenetics & Chromatin, 11*, 1-20.

Adhikari, A., Kim, W., & Davie, J. (2021). Myogenin is required for assembly of the transcription machinery on muscle genes during skeletal muscle differentiation. *PLoS One*, *16*(1), e0245618.

Blau, H. M., Pavlath, G. K., Hardeman, E. C., Chiu, C. P., Silberstein, L., Webster, S. G., Miller, S. C., & Webster, C. (1985). Plasticity of the differentiated state. *Science, 230*(4727), 758-766.

Bracken, A. P., Dietrich, N., Pasini, D., Hansen, K. H., & Helin, K. (2006). Genome-wide mapping of Polycomb target genes unravels their roles in cell fate transitions. *Genes & Development, 20*(9), 1123-1136.

Bratthauer, G. L. (2010). The avidin–biotin complex (ABC) method and other avidin–biotin binding methods. *Immunocytochemical methods and protocols*, 257-270.

Cao, Y., Kumar, R. M., Penn, B. H., Berkes, C. A., Kooperberg, C., Boyer, L. A., Young, R. A., & Tapscott, S. J. (2006). Global and gene specific analyses show distinct roles for Myod and Myog at a common set of promoters. *The EMBO journal, 25*(3), 502-511.

Caretti, G., Di Padova, M., Micales, B., Lyons, G. E., & Sartorelli, V. (2004). The Polycomb Ezh2 methyltransferase regulates muscle gene expression and skeletal muscle differentiation. *Genes & Development, 18*(21), 2627-2638.

Davis, R. L., Weintraub, H., & Lassar, A. B. (1987). Expression of a single transfected cDNA converts fibroblasts to myoblasts. *Cell, 51*(6), 987-1000.

Dilworth, F. J. (2022). JMJD3 activated hyaluronan synthesis drives muscle regeneration in an inflammatory environment. *Science, 377*(6606), 666-669.

Faralli, H., Wang, C., Nakka, K., Benyoucef, A., Sebastian, S., Zhuang, L., Chu, A., Palii, C. G., Liu, C., Camellato, B., Brand, M., Ge, K., & Dilworth, F. J. (2016). UTX demethylase activity is required for satellite cell–mediated muscle regeneration. *The Journal of Clinical Investigation, 126*(4), 1555-1565.

Fry, C. S., Porter, C., Sidossis, L. S., Nieten, C., Reidy, P. T., Hundeshagen, G., Mlcak, R., Rasmussen, B. B., Lee, J. O., Suman, O. E., Herndon, D. N., Finnerty, C. C. (2016). Satellite cell activation and apoptosis in skeletal muscle from severely burned children. *The Journal of Physiology, 594*(18), 5223-5236.

Goh, Q., & Millay, D. P. (2017). Requirement of myomaker-mediated stem cell fusion for skeletal muscle hypertrophy. *eLife, 6*, e20007.

Guitart, M., Lloreta, J., Mañas-Garcia, L., & Barreiro, E. (2018). Muscle regeneration potential and satellite cell activation profile during recovery following hindlimb immobilization in mice. *Journal of Cellular Physiology, 233*(5), 4360-4372.

Harrison, B. C., Allen, D. L., & Leinwand, L. A. (2011). IIb or not IIb? Regulation of myosin heavy chain gene expression in mice and men. *Skeletal muscle, 1*, 1-9.

Kassar-Duchossoy, L., Giacone, E., Gayraud-Morel, B., Jory, A., Gomès, D., & Tajbakhsh, S. (2005). Pax3/Pax7 mark a novel population of primitive myogenic cells during development. *Genes & development, 19*(12), 1426-1431.

Liu, Q. C., Zha, X. H., Faralli, H., Yin, H., Louis-Jeune, C., Perdiguero, E., Louis-Jeune, C., Perdiguero, E., Pranckeviciene, E., Muñoz-Cànoves, P., A. Rudnicki, M., Brand, M., Perez-Iratxeta, C., Dilworth, F. J. (2012). Comparative expression profiling identifies differential roles for Myogenin and p38α MAPK signaling in myogenesis. *Journal of molecular cell biology, 4*(6), 386-397.

Liu, Z., Wang, C., Liu, X., & Kuang, S. (2018). Shisa2 regulates the fusion of muscle progenitors. *Stem cell research, 31*, 31–41.

Luo, W., Li, E., Nie, Q., & Zhang, X. (2015). Myomaker, regulated by MYOD, MYOG and miR-140-3p, promotes chicken myoblast fusion. *International journal of molecular sciences, 16*(11), 26186-26201.

Mackey, A. L., Kjaer, M., Charifi, N., Henriksson, J., Bojsen-Moller, J., Holm, L., & Kadi, F. (2009). Assessment of satellite cell number and activity status in human skeletal muscle biopsies. *Muscle & Nerve: Official Journal of the American Association of Electrodiagnostic Medicine, 40*(3), 455-465.

Mauro, A. (1961). Satellite cell of skeletal muscle fibers. *The Journal of Biophysical and Biochemical Cytology, 9*(2), 493-495.

McKee, C. M., Chapski, D. J., Wehling-Henricks, M., Rosa-Garrido, M., Kuro-o, M., Vondriska, T. M., & Tidball, J. G. (2022). The anti-aging protein Klotho affects early postnatal myogenesis by downregulating Jmjd3 and the canonical Wnt pathway. *The FASEB Journal*, *36*(3), e22192.

Miller, K. J., Thaloor, D., Matteson, S., & Pavlath, G. K. (2000). Hepatocyte growth factor affects satellite cell activation and differentiation in regenerating skeletal muscle. *American Journal of Physiology-Cell Physiology, 278*(1), C174-C181.

Nakka, K., Hachmer, S., Mokhtari, Z., Kovac, R., Bandukwala, H., Bernard, C., Li, Y., Xie, G., Liu, C., Fallahi, M., Megeney, L. A., Gondin, J., Chazaud, B., Brand, M., Zha, X., Ge, K., & Dilworth, F. J. (2022). JMJD3 activated hyaluronan synthesis drives muscle regeneration in an inflammatory environment. *Science*, *377* (6606), 666-669.

Ohtani, K., Zhao, C., Dobreva, G., Manavski, Y., Kluge, B., Braun, T., Reiger, M. A., Zeiher, A. M., & Dimmeler, S. (2013). Jmjd3 controls mesodermal and cardiovascular differentiation of embryonic stem cells. *Circulation Research*, *113*(7), 856-862.

Robinson, D. C., & Dilworth, F. J. (2018). Epigenetic regulation of adult myogenesis. *Current Topics in Developmental Biology, 126*, 235-284.

Seale, P., Sabourin, L. A., Girgis-Gabardo, A., Mansouri, A., Gruss, P., & Rudnicki, M. A. (2000). Pax7 is required for the specification of myogenic satellite cells. *Cell, 102*(6), 777-786.

Seenundun, S., Rampalli, S., Liu, Q. C., Aziz, A., Palii, C., Hong, S., Blais, A., Brand, M., Ge, K. & Dilworth, F. J. (2010). UTX mediates demethylation of H3K27me3 at muscle-specific genes during myogenesis. *The EMBO Journal*, *29*(8), 1401-1411.

Sen, G. L., Webster, D. E., Barragan, D. I., Chang, H. Y., & Khavari, P. A. (2008). Control of differentiation in a self-renewing mammalian tissue by the histone demethylase JMJD3. *Genes & Development*, *22*(14), 1865-1870.

Tang, Q. Y., Zhang, S. F., Dai, S. K., Liu, C., Wang, Y. Y., Du, H. Z., Teng, Z. Q., & Liu, C. M. (2020). UTX regulates human neural differentiation and dendritic morphology by resolving bivalent promoters. *Stem Cell Reports*, *15*(2), 439-453.

Thieme, S., Gyárfás, T., Richter, C., Özhan, G., Fu, J., Alexopoulou, D., Muders, M. H., Michalk., Jakob, C., Dahl, A., Klink, B., Bandoła, J., Bachmann, M., Schrock, E., Buchholz, F., Stewart, A. F., Weidinger, G., Anastassiadis, K., & Brenner, S. (2013). The histone demethylase UTX regulates stem cell migration and hematopoiesis. *Blood, The Journal of the American Society of Hematology, 121*(13), 2462-2473.

Tidball, J. G. (2017). Regulation of muscle growth and regeneration by the immune system. *Nature Reviews Immunology*, *17*(3), 165-178.

von Maltzahn, J., Jones, A. E., Parks, R. J., & Rudnicki, M. A. (2013). Pax7 is critical for the normal function of satellite cells in adult skeletal muscle. *Proceedings of the National Academy of Sciences*, *110*(41), 16474-16479.

Wang, S., Sun, Y., Ren, R., Xie, J., Tian, X., Zhao, S., Li, X., & Cao, J. (2019). H3K27me3 depletion during differentiation promotes myogenic transcription in porcine satellite cells. *Genes*, *10*(3), 231.

Wehling-Henricks, M., Li, Z., Lindsey, C., Wang, Y., Welc, S. S., Ramos, J. N., Khanlou, N., Kuro-o, M., & Tidball, J. G. (2016). Klotho gene silencing promotes pathology in the mdx mouse model of Duchenne muscular dystrophy. *Human Molecular Genetics, 25*(12), 2465-2482.

Wen, Y., Bi, P., Liu, W., Asakura, A., Keller, C., & Kuang, S. (2012). Constitutive Notch activation upregulates Pax7 and promotes the self-renewal of skeletal muscle satellite cells. *Molecular and cellular biology*, *32*(12), 2300-2311.

White, J. P., Baltgalvis, K. A., Sato, S., Wilson, L. B., & Carson, J. A. (2009). Effect of nandrolone decanoate administration on recovery from bupivacaine-induced muscle injury. *Journal of Applied Physiology, 107*(5), 1420-1430.

Xia, Y., Ikedo, A., Lee, J. W., Iimura, T., Inoue, K., & Imai, Y. (2022). Histone H3K27 demethylase, Utx, regulates osteoblast-to-osteocyte differentiation. *Biochemical and Biophysical Research Communications*, *590*, 132-138.

Zammit, P. S., Golding, J. P., Nagata, Y., Hudon, V., Partridge, T. A., & Beauchamp, J. R. (2004). Muscle satellite cells adopt divergent fates: a mechanism for self-renewal?. *The Journal of Cell Biology*, *166*(3), 347-357.